

W62-39-011-002

SPACE RESEARCH COORDINATION CENTER

CASE FILE
COPY



N 7 1 - 3 2 2 9 5

NASA CR 119684

REACTIONS OF METASTABLE NITROGEN ATOMS

BY

CHORNG-LIEH LIN AND FREDERICK KAUFMAN

SRCC REPORT NO. 153

UNIVERSITY OF PITTSBURGH
PITTSBURGH, PENNSYLVANIA

JUNE 1971

The Space Research Coordination Center, established in May, 1963, has the following functions: (1) it administers predoctoral and postdoctoral fellowships in space-related science and engineering programs; (2) it makes available, on application and after review, allocations to assist new faculty members in the Division of the Natural Sciences and the School of Engineering to initiate research programs or to permit established faculty members to do preliminary; work on research ideas of a novel character; (3) in the Division of the Natural Sciences it makes an annual allocation of funds to the interdisciplinary Laboratory for Atmospheric and Space Sciences; (4) in the School of Engineering it makes a similar allocation of funds to the Department of Metallurgical and Materials Engineering and to the program in Engineering Systems Management of the Department of Industrial Engineering; and (5) in concert with the University's Knowledge Availability Systems Center, it seeks to assist in the orderly transfer of new space-generated knowledge in industrial application. The Center also issues periodic reports of space-oriented research and a comprehensive annual report.

The Center is supported by an Institutional Grant (NsG-416) from the National Aeronautics and Space Administration, strongly supplemented by grants from the A. W. Mellon Educational and Charitable Trust, the Maurice Falk Medical Fund, the Richard King Mellon Foundation and the Sarah Mellon Scaife Foundation. Much of the work described in SRCC reports is financed by other grants, made to individual faculty members.

REACTIONS OF METASTABLE NITROGEN ATOMS*

Chorng-Lieh Lin[†] and Frederick Kaufman

Department of Chemistry
University of Pittsburgh
Pittsburgh, Pa. 15213

Abstract

The line absorption technique was applied to the kinetic study of the two metastable atomic nitrogen states $N(2^2D)$ and $N(2^2P)$ in a flowing afterglow system. The optical absorptions of the NI 1493Å ($2p^3^2D - 3s^2P$) and 1743Å ($2p^3^2P - 3s^2P$) transitions were used for the quantitative measurement of $N(2^2D)$ and $N(2^2P)$ concentrations. Deactivation of $N(2^2D)$ and $N(2^2P)$ by the Pyrex tube wall was found to be very efficient *i.e.* occurs at nearly every collision. The second order rate constants at 300°K for the removal of $N(2^2D)$ by O_2 , N_2O , CO_2 , NO , N_2 , Ar and He were found to be $(6 \pm 2) \times 10^{-12}$, $(3.5 \pm 1.2) \times 10^{-12}$, $(5 \pm 2) \times 10^{-13}$, $(7 \pm 2.5) \times 10^{-11}$, $(1.6 \pm 0.7) \times 10^{-14}$, $(1 \pm 0.6) \times 10^{-16}$ and $\leq 1.6 \times 10^{-16} \text{ cm}^3 \text{ sec}^{-1}$, respectively. It was established that the process for the first three reactant gases results in chemical reaction rather than physical quenching.

I. Introduction

The recent rapid advances in the study of electronically excited metastable "air" species have derived their impetus from experimental and theoretical investigations of planetary atmospheres. But whereas there has been a profusion of work on $O(^1D)$ and $O(^1S)$ and $O_2(^1\Delta_g)$ and $O_2(^1\Sigma_g^+)$, not much information is available on the N-metastables, 2^2D^0 and 2^2P^0 , although

the former is very probably the precursor of most of the NO in the earth's mesosphere and thermosphere.¹ These two states lie 2.38 and 3.58eV above the 4S ground state and their substates $2D_{5/2}$, $^2D_{3/2}$, $^2P_{1/2}$, and $^2P_{3/2}$ have radiative lifetimes of 40hr, 17hr, 12sec, and 12sec, respectively.² They are connected by strongly allowed transitions to a common upper state $2p^23s\ ^2P_{1/2, 3/2}$, and these give rise to the multiplets near 1493 and 1743Å which were used in the present study to measure the metastable densities in absorption. Evidence for the presence of these species in the upper atmosphere comes from airglow experiments in which spectral lines at 5200Å ($2^2D^0 - 2\ ^4S^0$)³⁻⁶, 3466Å ($2\ ^2P^0 - 2\ ^4S^0$)^{4, 7}, 10,400Å ($2^2D^0 - 2^2P^0$)⁴, 1493Å ($3^2P - 2^2D^0$)⁸⁻¹⁰, and 1743Å ($3^2P - 2^2P^0$)¹⁰ were observed. In their study of the nebular transition at 5200Å, Wallace and McElroy⁵ and Hernandez and Turtle³ suggested quenching rate constants of $N(^2D)$ by O_2 of the order of $10^{-12} \text{cm}^3 \text{sec}^{-1}$. In the laboratory, N -metastable, have been detected by mass spectrometry,¹¹ optical spectrometry,¹²⁻¹⁴ and electron spin resonance,¹⁵ but the only quantitative kinetic study of $N(^2D)$ reactions or quenching has been that by Black *et al.*¹⁶ who monitored the decay of the β -bands of $NO(B^2\pi - X^2\pi)$ produced by the reaction of $N(^2D)$ with N_2O as earlier proposed by Welge,¹⁷ following the vacuum ultraviolet photolysis of N_2O .

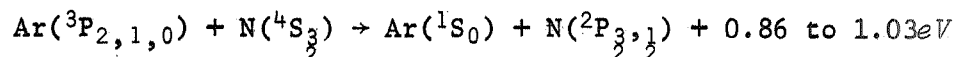
In this work we measured directly the decay of $N(^2D)$ and $N(^2P)$ produced by microwave discharges in a flow system by line absorption of the 1493Å and 1743Å transitions. Moreover, we also measured quantitatively the appearance of O atoms produced directly or indirectly in reactions of $N(^2D)$ with several oxygen-containing reactants, and have thus resolved the question of whether physical quenching or chemical reactions are actually taking place. Our preliminary results¹⁸ concerning the reaction of $N(^2D)$ with O_2 have been used by Norton and Barth¹⁹ and by Strobel *et al.*²⁰

in their model calculations of NO density profiles in the upper atmosphere. These calculations are in good agreement with the rocket measurements of Barth^{21a} and Meira^{21b}.

II. EXPERIMENTAL

A. Apparatus:

The light source and flow absorption cell which is shown schematically in Figure 1 have been described previously. To measure the concentrations of N(²D) and N(²P), the apparent 1493Å doublet (actually a triplet consisting of two close lines at 1492.62Å and 1492.81Å and one at 1494.67Å) and the apparent 1743Å doublet (A quartet, consisting of two pairs of unresolved lines at 1742.72Å and 1742.73Å and at 1745.25Å and 1745.26Å) were used as light sources which were excited in flowing He or Ar containing a trace of N₂ at a pressure of 1 Torr. Normally the stronger lines of both doublets, *i.e.* at 1492Å and 1742Å, were used because they provide larger absorption than their respective counterparts. The weaker lines were used occasionally for checking the experimental data. Both doublets are easily excited in the microwave discharge and have much greater intensities than the resonance triplet. Intensity ratios very close to the theoretical value of 2 to 1 were usually obtained for the two lines of either doublet indicating that the populations of N(²D) and (²P) in the source were not large. He-N₂ light sources were used mainly, because the lines excited by Ar-N₂ discharges were found to be absorbed to a lesser extent than those excited in flowing He-N₂ at the same concentrations of N(²D) or (²P). This is probably due to energy transfer processes such as



occurring in Ar-N₂ sources. The excited N-atoms would then have 0.64 to 0.76eV excess kinetic energy and give rise to broadened emission lines, as had been observed earlier in rare gas-oxygen sources.²² The emission lines traversed the absorption cell where they were partially absorbed by N(²D) or N(²P) atoms, which were produced upstream by a microwave discharge in flowing He or Ar containing a small amount of added N₂, and detected by a vacuum monochromator (Jarrell-Ash, Fastie-Ebert, 0.5 meter).

Cylinder grades of He, Ar, N₂, O₂ and N₂O were used without further purification. CO₂ was prepared from dry ice by repeated pumping and cooling to 77°K followed by sublimation while immersed in a dry ice-isopropanol bath. NO was purified by slow passage over supported NaOH at atmospheric pressure, condensation at 77°K, and repeated sublimation.

In order to find absorption flow and discharge conditions which would maximize N(²D) and (²P) concentrations while maintaining the gas temperature as reproducible as possible, the flow rate of N₂ and carrier gas as well as discharge power were varied. Gas temperatures were measured using either a mercury thermometer or thin bare iron-constantan thermocouples inserted in the tube at various distances from the discharge. Under low power (<20W) discharge conditions which were employed throughout the experimental study of N(²D), the gas temperature decayed to ambient room temperature within less than 15cm distance for all conditions of He flow and for low pressure (<3.2 Torr) Ar flow. All rate measurements for N(²D) were thus made in the cooler zones of the absorption tube *i.e.* near 300°K except for some experiments employing high pressures of Ar at about 310°K. For the studies of N(²P), higher power is required to produce adequate concentrations so that temperatures in the reaction zone were typically about 400°K. The flow velocities at 10 Torr

pressure were about 5000cm/sec for Ar and 5500cm/sec for He.

Two methods were employed to study the quenching rates by various gases; one by moving the discharge cavity along the tube to different distances with respect to the fixed spectrometer position while measuring the absorption of the 1492\AA and 1742\AA lines for each cavity position, and the other by keeping the discharge at some fixed upstream position while introducing varying amounts of reactant gas through a multiperforated teflon loop inlet and measuring the decay of $\text{N}(^2\text{D})$ and (^2P) atoms as function of added reactant concentration.

The former method was used for estimating the quenching rates at the tube wall and by carrier gases. The decay curves for the metastables at various pressures, up to 15.9 Torr, were obtained by changing the flow rates of Ar or He while maintaining a small constant N_2 flow. Care was taken to move the discharge cavity from one position to another in such a manner that its discharge parameters (cavity geometry and tuning) remained unaltered. The quenching rate by N_2 was measured by varying the flow rate of added N_2 in a large constant flow of carrier gas and alternately by adding variable amounts of N_2 through the teflon inlet. Since the flow rate of carrier gas was much greater than that of N_2 , constant pressure could be maintained.

Quenching rates by gases other than the carrier gas were measured by introducing the reactant gases through the teflon inlet situated 10.6cm upstream of the spectrometer window. The reaction zone is so short that the viscous pressure drop was found to be negligible, <4%. Since the loss of metastables by wall deactivation is nearly inversely proportional to the total pressure, a relatively high pressure is needed to maintain a workable metastable concentration with the present detection system. He

and Ar pressures from 6.8 Torr to 15 Torr containing 0.5% to 4.3% of N_2 were usually employed in the experimental measurements.

B. Metastable Concentration Measurement

The relation between the fractional absorption, $A_\alpha \equiv (I_0 - I)/I_0$, and the optical depth, $k_0 \ell$, for a single line in the Doppler-Doppler approximation is given in Mitchell and Zemanski.²³

For an unresolved multiplet the relation becomes

$$A_\alpha = 1 - \frac{\left\{ \sum_i \int_{-\infty}^{\infty} C_i \exp \left[-\left(\frac{\omega_i}{\alpha_i} \right)^2 \right] \exp \left[-\left(\ell \sum_j k_{0j} e^{-\omega_j^2} \right) d\omega_i \right] \right\}}{\sum_i \int_{-\infty}^{\infty} C_i \exp \left[-\left(\frac{\omega_i}{\alpha_i} \right)^2 \right] d\omega_i} \quad (1)$$

where $i, j = 1, 2, \dots$ serves as the index of the lines within the multiplet, and all other symbols have been defined in Ref. 23 and in our earlier paper.²² The constants C_i are proportional to the emission intensities and the denominator is $\pi^{1/2} \sum_i C_i \alpha_i$.

For the three lines of the $2^2D^0 - 3^2P$ transition, the sum rules based on LS coupling require that the line intensities stand in the ratio 9:1:5, that the corresponding absorption f -value are in the ratio 6:1:5, and the peak absorption coefficients, k_0 , are like 9:1:5. For the unresolved NI 1492Å doublet, the first two of the three lines, both the absorption coefficients and intensities for the 1492.62Å and 1492.81Å lines therefore have ratios of 9:1 so that we may set $k_{02} = \frac{1}{9} k_{01}$ and

and $C_2 = \frac{1}{9} C_1$ where subscripts 1 and 2 denote the 1492.62Å and 1492.81Å lines, respectively.

A_α was evaluated by computer as a function of $k_{o1} \ell$, the absorption coefficient of the stronger component, using $\alpha_1 = \alpha_2 = \sqrt{2}$ since the temperature of the light source is approximately 600°K²² and that of the absorber gas is clearly 300°K.

Similarly, for the $2^2P^0 - 3^2P$ transition, the line intensities are like 1:5:2:1, the f -values like 2:5:4:1, and the k_o like 1:5:2:1 for the four lines of increasing wavelength as given above. For the unresolved NI 1742Å doublet we set $k_{o2} = \frac{1}{5} k_{o1}$ and $C_2 = \frac{1}{5} C_1$, and again $\alpha_1 = \alpha_2 = \sqrt{2}$, where subscript 1 refers to the stronger line of the doublet, *i.e.* 1742.73Å. Since $k_o \ell$ is proportional to the absorber concentration, the concentration of N(²D) and (²P) corresponding to a certain value of $k_o \ell$ can be calculated if the f -value is known. For the 1492Å line. The relation is

$$f_{LU} = 2.67 \times 10^{11} \frac{k_o}{N_L} \quad (2)$$

and for the 1742Å line

$$f_{LU} = 2.29 \times 10^{11} \frac{k_o}{N_L} \quad (3)$$

The radiative lifetime for the common upper state (3^2P) of these two transitions was measured by Lawrence and Savage²⁴ using the phase shift method and the multiplet A coefficients given by them were based on the branching ratio of the two multiplets given in the NBS tabulation.² The

NBS listing of f -values and A-coefficients for the multiplets was taken from values given by Labuhn²⁵ from his arc experiments. We did not adopt Labuhn's value for the calculation of the $N(^2D)$ and $N(^2P)$ concentration because his values are generally considered to be too high as shown from the comparison of his OI and NI resonance triplet data with recent literature values.²² It should also be pointed out that the NBS f -values² for the $3^2P - 2^2D^0$ multiplet based on Labuhn's measurements do not obey the sum rule sufficiently closely, and that the wavelength of the third line is 1492.81 rather than 1492.67Å. The lifetime measurements²⁴ lead to absorption f -values of 0.078, 0.013, and 0.065 rather than the listed² 0.12, 0.019, and 0.084. For the $3^2P - 2^2P^0$ multiplet, f -values of 0.021, 0.053, 0.043, and 0.011 were adopted based on Ref. 24 rather than the listed 0.032, 0.082, 0.059, and 0.015. Because of the small energy splitting in the $2D^0$ state (9.2cm^{-1}) and the negligible splitting in the $2P^0$ state, the populations of their sub-states are proportional to their statistical weight. Total concentrations of metastables were obtained in either of two equivalent ways: From k_{01} using Equation (2) with $f_{LU} = 0.078$ and $N_L = 0.6[^2D]$ (because of the 6:4 statistical weights of the $J = \frac{5}{2}$ and $\frac{3}{2}$ substates), or from the total $k_0 = k_{01} + k_{02} = \frac{10}{9} k_{01}$ with an average f -value, $\sum_L g_L f_{LU} / \sum g_L$, and $N_L = [^2D]$. The k_0 in the subsequent text and figures is the total k_0 and should be used with the average f -value (0.052 for the 2D doublet at 1492Å) and with the total metastable concentration in Equation (2) or (3).

In normal experimental conditions with low discharge power, the concentration of $N(^2D)$ in the absorption cell was less than $2.4 \times 10^{12} \text{cm}^{-3}$ and that of $N(^2P)$ less than $4 \times 10^{11} \text{cm}^{-3}$. The ground state atomic nitrogen concentration was estimated to be of the order of 1 to $2 \times 10^{14} \text{cm}^{-3}$ by

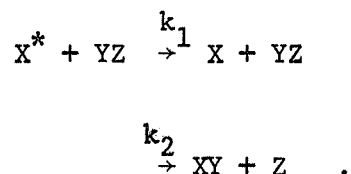
titration of N with NO to the visual endpoint or to zero absorption of the 1200Å resonance triplet.

C. The Flow Equations

As will be shown later, the decay of $N(^2D)$ and $N(^2P)$ in flowing Ar or He containing traces of N_2 is mainly diffusion-controlled, *i.e.* the quenching rates by carrier gases and by N_2 are negligible in comparison with that by the wall. If we assume that all N metastables are produced in the discharge and that there are two major mechanisms responsible for the decay of metastable atoms, namely, the diffusion of metastables, X^* , to the wall and chemical reaction with reactant gas, YZ, then the rate of change of metastables is given by

$$u \frac{\delta n}{\delta x} = D \nabla^2 n - k N n \quad (4)$$

where D is the diffusion coefficient of X^* and assumed to be constant, u is the flow velocity, x is the axial coordinate, n is the concentration of X^* , N is the concentration of the reactant gas YZ and k is the total rate constant for quenching and/or chemical reaction



Since transport along the axial direction by convection is much faster than by diffusion, we need only consider radial diffusion. Equation (4) then becomes

$$u \frac{\delta n}{\delta x} = \frac{D}{r} \frac{\delta}{\delta r} \left(r \frac{\delta n}{\delta r} \right) - k N n \quad (5)$$

Reynolds numbers are less than 70 for He and less than 500 for Ar, well below the onset of turbulence. Consequently, the velocity profile can be expressed as

$$u(r) = 2 u_o \left(1 - \frac{r^2}{r_o^2}\right) \quad (7)$$

Substituting in Equation (5), the lowest mode solution²⁶⁻³⁰ is now

$$\bar{n}(x) = n_o \exp \left\{ -\left[\frac{D\lambda_o^2}{2 r_o^2} + \left(\frac{1 + \epsilon_1}{2} \right) k N \right] \frac{x}{u_o} \right\} \quad (8)$$

where $\lambda_o = 2.710$ and $\epsilon_1 = 0.237$ as given by Cher and Hollingsworth.²⁷ This is in good agreement with the result obtained by Ferguson *et al.*²⁸ with $\epsilon_1 = 0.230$ whereas Huggins and Cohn²⁶ and Farragher³⁰ gave a somewhat higher value of 0.258. Equations (8) and (6) are similar except for the empirical constants associated with the diffusion and reaction terms. Thus the diffusion coefficients and rate constants obtained based on Equation (6) have to be increased by factors of 1.58 and 1.62, respectively, if the planar flow model (Equation 6) is used.

III. RESULTS

A. The Rate Constants

Typical decay curves of $N(^2D)$ at various pressures of inert gas ($\leq 43\%$ of N_2 in Ar) are plotted in Figure 2 as $k_o t$ vs. time. The corresponding first order rate constants are listed in Table 1 as a

function of pressure. Similar data for $N(^2D)$ in He are listed in Table 2 and for $N(^2P)$ in Table 3. k^I contains mainly two contributions, one from the diffusion of the metastables to the wall followed by surface deactivation and the other from volume deactivation by carrier gas. These correspond to the two terms in the right hand side of Equation (6). At low pressures, the decay will be governed entirely by diffusion and the contribution from quenching by constituent gases will be negligible. Since diffusional quenching is inversely proportional to and deactivation by carrier gas is directly proportional to the pressure, a plot of $k^I P$ against P^2 should yield a straight line with its slope equal to the second order quenching rate constant for carrier gas and its intercept equal to the first order rate constant due to diffusion at unit pressure, k_d^I , which is equal to $\frac{D_o \gamma_o^2}{r_o^2}$ in Equation (6) where D_o is the diffusion coefficient at 1 Torr.

$k^I P$ in Table 2 is nearly constant with an average value of $8000 \text{ sec}^{-1} \text{ Torr}$ indicating that diffusional quenching is dominant and that deactivation by He is negligible even at a pressure as high as 15.8 Torr. If we ascribe the decay of $N(^2D)$ in He wholly to diffusional quenching, then $k_{d, \text{He}}^I = 8000 \text{ sec}^{-1} = \frac{D_o \gamma_o^2}{r_o^2} = 16 D_o$, since the radius of the tube is 0.6cm, giving a value of $D_o^{\text{He}} = 500 \text{ cm}^2/\text{sec}$. Multiplying by the correction factor of 1.58, D_o^{He} becomes $790 \text{ cm}^2/\text{sec}$ in good agreement with the value of $700 \text{ cm}^2/\text{sec}$ reported by Morgan and Schiff³¹ for O in He. This means that surface deactivation is very efficient *i.e.* occurs at nearly every collision. If at most 10% of k^I is due to quenching by He, an upper limit of $1 \times 10^{-16} \text{ cm}^3/\text{sec}$ can be assigned to $k_{N(^2D), \text{He}}^{II}$.

For the Ar case, the diffusion is about a factor of three slower than in He and there is a slight increase of k^{I}_{P} with increasing pressure in Table 1. Plots of k^{I}_{P} against P^2 in Figure 3 yield values of $D_{\text{O}}^{\text{Ar}} \approx 270 \text{ cm}^2/\text{sec}$ and $k^{\text{II}}_{\text{N}(^2\text{D}), \text{Ar}} \approx 1 \times 10^{-16} \text{ cm}^3 \text{ sec}^{-1}$. The D_{O}^{Ar} value is again close to the literature value of $209 \text{ cm}^2/\text{sec}$ for atomic oxygen.³¹

Similar treatment of the data for $\text{N}(^2\text{P})$ in Table 3 results in $D_{\text{O}}^{\text{Ar}} \approx 330 \text{ cm}^2/\text{sec}$ for $\text{N}(^2\text{P})$ and $k^{\text{II}}_{\text{N}(^2\text{P}), \text{Ar}} \approx 7 \times 10^{-16} \text{ cm}^3 \text{ sec}^{-1}$, a factor of 7 higher than the $\text{N}(^2\text{D})$ value.

To obtain the quenching rate constant of $\text{N}(^2\text{D})$ by N_2 , a series of experiments were done by varying the flow of N_2 in a very large flow of He or Ar, typically at 14.7 Torr of He or 6.8 Torr of Ar as shown in Figure 4. The first order rate constants are plotted in Figure 5 against the partial pressure of N_2 , P_{N_2} . The slopes in Figure 5 give a value of $k^{\text{II}}_{\text{N}(^2\text{D}), \text{N}_2} \approx 1.6 \times 10^{-14} \text{ cm}^3 \text{ sec}^{-1}$ when the laminar flow correction is applied.

The introduction of reactant gases through the perforated teflon inlet 10.6 cm above absorption cell to react with metastable atomic nitrogen produced 26 cm (in some cases 19.5 cm or 32.5 cm) above the absorption cell was the primary means of obtaining rate coefficients in this study. The slope of the decay curve plotted as $\log(k_0 \ell)$ against added reactant gas concentration is equal to $-k^{\text{II}}_t/2.3$ from which the second order rate constant k^{II} was obtained. The decays of $\text{N}(^2\text{D})$ and $\text{N}(^2\text{P})$ were also measured with N_2 added through the inlet and yielded values for $k^{\text{II}}_{\text{N}(^2\text{D}), \text{N}_2} \approx 2 \times 10^{-14} \text{ cm}^3/\text{sec}$ at 310°K and $k^{\text{II}}_{\text{N}(^2\text{P}), \text{N}_2} \approx 6 \times 10^{-14} \text{ cm}^3/\text{sec}$ at 400°K , respectively. The former agrees well with that obtained from the earlier method by variations of N_2 partial pressure in a large flow of carrier gas. The latter is in contradiction with the conclusions of

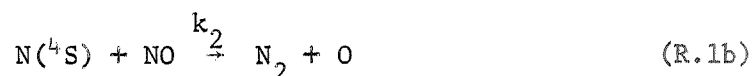
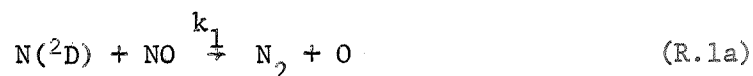
Noxon¹³ who reported a quenching rate constant of the order of 10^{-19} cm³/sec.

Figures (6), (7) and (8) show the decay of N(²D) in He and Ar with added O₂, N₂O and CO₂ and their corresponding rate constants are given in the second column of Table 4, assuming the simple constant flow model of Equation (6). Contrary to this prediction, the present data show some discrepancy between the k's of He and Ar experiments, especially when the rate constants are small.

The origin of this discrepancy is somewhat obscure, but it is very likely due to an inlet effect. For the slow reactions, relatively large quantities of added reactant gas are required to produce a significant decrease in absorption. If, because of imperfect point or plane source geometry, the radial diffusion of metastables to the wall is perturbed, a small change in that loss term may be of the same magnitude as the homogeneous loss term due to added gas. It does seem clear, moreover, that in view of the short reaction length, the gross perturbation of the laminar flow by the fairly large inlet tube, and the non-planar reactant gas addition, the correction factor by which the slope of the log ($k_0 \ell$) vs. added gas concentration is to be multiplied must be somewhere between 1.0 (constant velocity) and 1.62 (parabolic velocity profile). Arbitrarily, a mean value of 1.3 has been adopted by which the average of the He and Ar rate constants is multiplied and shown in Column 4 of Table 4. The corresponding error limits have also been widened to take account of the larger uncertainty. The full correction factor of 1.6 was used in the last two rows of Table 4, because no gas addition was made through the inlet tube in the $k_{\text{He and Ar}}^{\text{II}}$ experiments.

For the reaction of N(²D) with NO, the determination of the rate constant was different from the previous reactions whose rate

constants are based on Equation (6), because of the presence of large concentrations of ground state atomic nitrogen which also reacts with NO with great speed. Therefore, there are two parallel reactions responsible for removal of NO, namely



The rate equation for the decay of $\text{N}(^2\text{D})$ will now be

$$-\frac{d[{}^2\text{D}]}{dt} = k_1 [{}^2\text{D}] [\text{NO}] + k_w [{}^2\text{D}] \quad (9)$$

where $[{}^2\text{D}]$ is the concentration of $\text{N}(^2\text{D})$. Integration of Equation (9) from $t = 0$ to t results in

$$-\ln \frac{[{}^2\text{D}]}{[{}^2\text{D}]_0} = k_1 \int_0^t [\text{NO}] dt + k_w t \quad (10)$$

where $[{}^2\text{D}]_0$ is the initial concentration of $\text{N}(^2\text{D})$ and k_w is the first order rate constant of wall deactivation. In the present experiments, t is known from the flow velocity, NO is varied *i.e.* added to the reaction tube at different flow rates, and the equation can be re-written as

$$-\ln[{}^2\text{D}] = k_1 \int_0^t \{ [\text{NO}]_0 - x \} dt + \text{constant} \quad (11)$$

where $[\text{NO}]_0$ is the initial NO concentration and x is the concentration of NO reacted. Plots of $\ln[{}^2\text{D}]$ vs. $\{ [\text{NO}]_0 t - \int_0^t x dt \}$ have a slope of k_1 . Since $[\text{N}({}^4\text{S})] \gg [\text{N}({}^2\text{D})]$, we can calculate x from the integrated second order rate equation of the $\text{N}({}^4\text{S}) + \text{NO}$ reaction,

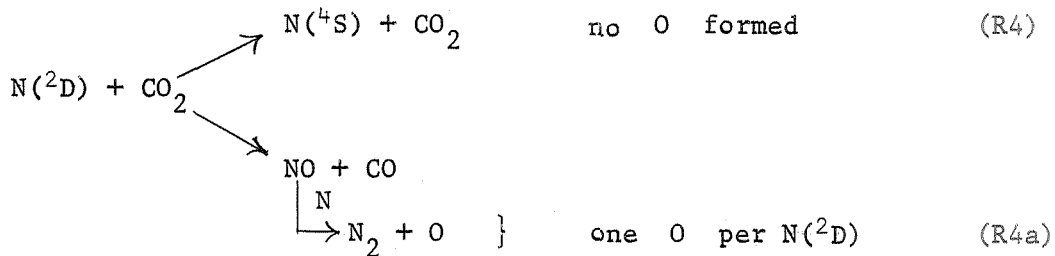
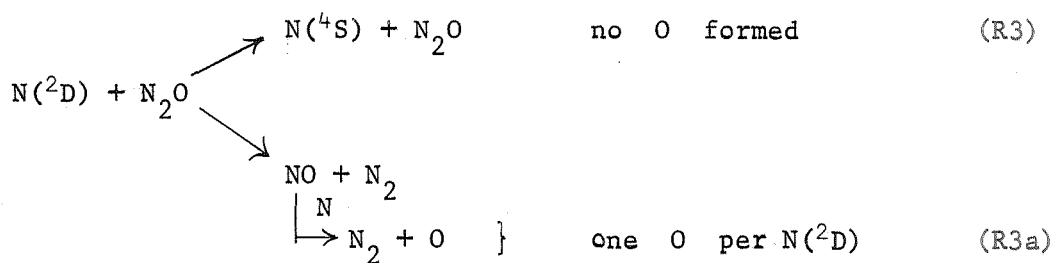
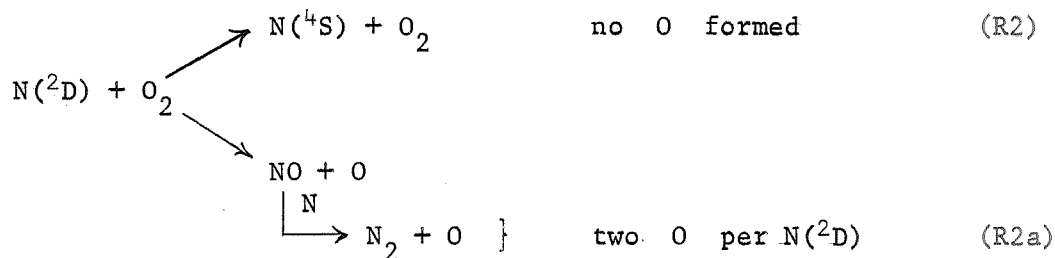
$$\frac{1}{a-b} \ln \frac{b(a-x)}{a(b-x)} \approx k_2 t \quad (12)$$

where a is the initial $\text{N}({}^4\text{S})$ concentration and b the initial concentration of added NO. a was measured by visual titration with NO and the integration of $\int_0^t x dx$ was done by computer assuming $k_2 = 3 \times 10^{-11} \text{cm}^3 \text{sec}^{-1}$, a rate constant which is well known and was discussed previously.²² A typical plot of $\log k_0$ against $[\int_0^t (\text{NO}) dt]$ is shown in Figure 9 and the rate constant is given in Table 4.

B. Reaction or Quenching?

The question of reaction or quenching for some of the reactions studied is important in upper atmosphere chemical kinetics, especially for $\text{N}({}^2\text{D}) + \text{O}_2$, since the large NO concentration found in the upper atmosphere may come from this reaction. To clarify this question for the reactions of $\text{N}({}^2\text{D})$ with O_2 , N_2O , or CO_2 , we have detected the reaction products quantitatively by monitoring the O-atom production rate against reactant gas concentration. In each of the following three

processes the upper arrow represents physical quenching and the lower arrow chemical reaction.



In the case of $\text{N}(^2\text{D})$ quenching, no O-atoms would be formed. If reaction did occur, the $\text{N}(^2\text{D}) + \text{O}_2$ reaction is capable of producing two O-atoms.

for each $N(^2D)$ because of the rapid $NO + N(^4S) \rightarrow N_2 + O$ reaction, whereas for the $N(^2D) + N_2O$ or $N(^2D) + CO_2$ reactions, one O-atom could be produced. The O-atom production due to the reactions between ground-state N and the reactant gases is known to be very slow at 300°K. This was confirmed by measuring the O-atom production due to reaction with ground state N-atoms alone. Here $N(^4S)$ was produced by placing the microwave discharge 70cm above the spectrometer window which assures the complete decay of metastables before reactant addition.

To measure the O-atom concentration produced in the reactions, the strongest line ($1302\overset{\circ}{A}$) of the OI resonance triplet was used as the light source and was excited in the same way as in the measurements of the OI f -value.²² Figure 10 shows the value of $k_O l$ for the $1302\overset{\circ}{A}$ line plotted against the concentration of added O_2 . The apparent $k_O l$ contains the absorption due to reactant gas itself as well as that due to O-atoms produced from the reaction when the microwave discharge was placed 70cm upstream, *i.e.* due to the reaction involving ground state N-atoms alone. These contributions were subtracted from the apparent $k_O l$ and the residual $k_O l$ is regarded as entirely due to the absorption by O-atoms resulting from the reaction of $N(^2D)$ and $N(^2P)$ with reactant gas. These corrected $k_O l$ were then converted to O-atom concentration and are plotted in Figure 11 as function of O concentration. Similar data were plotted for N_2O and CO_2 additions. The $N(^2P)$ contribution to the O-atom production was estimated from Equation (3) and absorption at $1742\overset{\circ}{A}$, and subtracted from the total O-atom curves. The "true" fractional O-atom yields, (dotted curve) *i.e.* $[O]_{\text{produced}} / [N(^2D)]_{\text{reacted}}$ for large reactant addition, were found to be 2.4, 1.3, and 1.05 for O_2 , N_2O and CO_2 , respectively, and agree reasonably well with the stoichiometric ratios 2, 1, and 1

from the reaction schemes (R2 to 4). The slight excess of these ratios above the theoretical value may be due to incorrect f -values for the $N(^2D$ and $^2P)$ lines or it may arise from concurrent reactions of species such as vibrationally excited N_2 molecules, N_2^{\dagger} , with added reactant. Kretschmer and Petersen³² reported, for example, that at short times after a N_2 discharge, when the N_2 vibrational temperature was high, the dissociation reaction $N_2^{\dagger} + O_2 \rightarrow N_2 + O + O$ occurred. However, with our discharge conditions of small N_2 to carrier gas ratios, the N_2^{\dagger} concentration should be small since no characteristic "pink glow" was ever observed. The agreement of our measurements with the stoichiometric values thus indicates that the three processes represent quantitative reaction rather than quenching.

IV. DISCUSSION

It is an important assumption in the derivation of the flow equations that the N-metastables are produced only in the discharge and not in the afterglow. This is valid because firstly, the decay curves in Figure 2, where traces of N_2 in various flows of carrier gas were discharged showed a first order decrease along the tube, indicating that there was no further source term after the discharge and the decay curves in Figure 4, where the partial pressure of N_2 was varied in a large constant flow of carrier gas through the microwave discharge, also showed the expected linear semilog plot of $k_0 l$ vs. time; secondly, the emission at 1200Å and 1492Å coming from the afterglow in the absorption cell was measured for various discharge to absorption cell distances with the light source turned off. Weak emission was observed at very small distances, dropping rapidly to zero as the distance was

increased. This may be taken as slight additional evidence that strong source terms are absent in the afterglow.

It has been shown here that the decay of $N(^2D)$ in flowing afterglows of He or Ar containing small amounts of N_2 is primarily due to wall deactivation. The reason that N-metastables survive from the discharge in large flows of inert gas with small flows of N_2 , but not in pure nitrogen is that the quenching rate constants by He and Ar are at least two orders of magnitude small than that by N_2 . This result is in accord with the findings of Foner and Hudson¹¹ whose mass spectrometrically measured $N(^2D)$ and (^2P) concentrations in a discharge of 1.8 Torr of pure N_2 were two orders of magnitude smaller than those from a discharge in 2.2 Torr He with 0.016 Torr of N_2 . For the latter they reported concentration ratios of $N(^4S): N(^2D): N(^2P) = 100:17:6$ sampled 1 msec after leaving the discharge as against our ratios of about 100:4.0:1.3 at similar flow conditions, but at lower power.

The present rate constants were mainly obtained in experiments in which reactant gases were introduced through a teflon loop inlet 15.5cm below the discharge cavity. This distance corresponds to a flow time of about 3 msec under normal experimental conditions. One must then consider that, in addition to all of the species examined so far, electronically excited states of N_2 and He (or Ar), most likely $N_2(A^3\Sigma_u^+)$ and He(3S) or Ar(3P), are probably also present in the immediate discharge afterglow and may interfere with the kinetics. $N_2(A^3\Sigma_u^+)$ has been studied by Dugan³³ in an N_2 discharge afterglow, and its concentration sampled 9 msec downstream at a pressure of 7 Torr was reported to be less than $2 \times 10^{12} \text{ cm}^{-3}$. Deactivation by $N(^4S)$ was found to be the major deactivation process for which several investigators³⁴ have reported

a rate constant of about $5 \times 10^{-11} \text{ cm}^3/\text{sec}$. With ground state N concentrations of 1 to $2 \times 10^{14} \text{ cm}^{-3}$ in the afterglow, the $\text{N}_2\text{-A}$ state will be destroyed within a few milliseconds. Though there is recent evidence^{34c} that this deactivation reaction produces $\text{N}(^2\text{P})$, such a source term of metastables is quite small if it is assumed that in the afterglow the $\text{N}_2\text{-A}$ -state is formed principally as the product of the chemiluminescent recombination of $\text{N}(^4\text{S})$ in the 1st positive system of N_2 . The second-order chemiluminescent rate constant is about $10^{-17} \text{ cm}^3 \text{ sec}^{-1}$ which makes this source term about $10^{11} \text{ cm}^{-3} \text{ sec}^{-1}$ compared with observed loss rates of 10^{13} to $10^{14} \text{ cm}^{-3} \text{ sec}^{-1}$. $\text{He}(^3\text{S})$ concentrations have been measured by Huggins and Cahn²⁶ under similar discharge flow conditions as ours (He flow velocity $5 \times 10^3 \text{ cm/sec}$ in 1 cm diameter tube) who found peak densities close to the discharge cavity of less than $1.8 \times 10^{11} \text{ cm}^{-3}$ at He pressures between 1.5 and 20 Torr and the densities were found to decay exponentially along the tube. $\text{He}(^3\text{S})$ is known to have fast Penning ionization reactions³⁵ with O_2 and N_2 ($k_{\text{O}_2} \sim 5 \times 10^{-10}$ and $k_{\text{N}_2} \sim 1.4 \times 10^{-10} \text{ cm}^3/\text{sec}$) resulting in the excited molecular ions O_2^{+*} which emit an intense bright yellow-green flame owing to the excitation of both the first negative system of O_2^+ ($b^4\Sigma_g^- \rightarrow a^4\Pi_u$) and the second negative system of O_2^+ ($A^2\Pi_u \rightarrow X^2\Pi_g$) and an intense bright blue flame due to the first negative system of N_2^+ ($B^2\Sigma_u^+ \rightarrow X^2\Sigma_g^+$). No blue flame was ever observed in the afterglow indicating that $\text{He}(^3\text{S})$ concentrations are small. The possible reaction of $\text{He}(^3\text{S})$ with O_2 molecules was also checked by introducing O_2 through a teflon inlet 15.5 cm below the discharge cavity into the reaction zone in 15 Torr of pure He. Neither O-atom production nor a yellow green flame was ever observed. In the case of Ar, because of the lower energy of the $\text{Ar}(^3\text{P})$ metastable state, we may expect a larger metastable

concentrations, but, since the reactant gas concentrations are large, the loss of reactant molecules can be neglected. The ground state N-atom reactions with reactant gases studied are too slow to be important except in the case of added NO where the reaction has been taken into account in the derivation of the rate equation. Therefore, the application of Equation (6) to this study is, in general, justified. The general agreement of our results with those of Black *et al.*¹⁶ who studied the vacuum *u.v.* photolysis of N₂O in the presence of added gases (Column 5 of Table 4) is, for the most part, astonishingly good. For the three important reactions with O₂, N₂O, and CO₂, the agreement is well within the error bars of the two investigations. For N₂ our rather imprecise value for *k* is a little more than twice theirs whereas for NO, where there is competition with the much greater net rate of the N(⁴S) + NO reaction, theirs is a little over a factor two greater than ours. Even in those very difficult applications the rate constant is well established to within a factor of two. The three reactions of ground state atomic nitrogen with O₂, N₂O and CO₂ have been found to be very slow. Wilson's³⁶ ESR result for $k_{O_2} = 2.4 \times 10^{-11} e^{-7.9 \text{ kcal/RT}} \text{ (cm}^3/\text{sec)}$ which is in excellent agreement with Schofield's³⁷ composite of old data, $2.5 \times 10^{-11} \exp(-7.8/\text{RT})$ gives a rate constant of $5.3 \times 10^{-17} \text{ cm}^3/\text{sec}$ at 300°K. Kistiakowsky and Volpi³⁸ reported $k_{N_2O} \leq 2 \times 10^{-16}$ at 553°K. Herron and Huie's³⁹ mass spectrometric study of the CO₂ reaction gave $k_{CO_2} \leq 1.6 \times 10^{-16}$ at 550°K. The slowness of the last two reactions is undoubtedly due to their failure to conserve spin. The substitution of N(²D) for N(⁴S) in the above reactions thus increases the rate constants at 300°K by three to five orders of magnitude, probably because it removes their spin forbiddenness and provides additional reaction channels due to their much greater exothermicities.

* Supported by the Defense Atomic Support Agency and monitored by the U. S. Army Research Office-Durham under Grant DA-ARO-D-31-124-70-G49.

† Submitted in partial fulfillment of the requirements for the Ph.D. degree. Present address: Jet Propulsion Laboratory, California Institute of Technology, Pasadena, California 91103.

REFERENCES

1. a. F. Kaufman, Reference 19 in a paper by T. M. Donahue, Invited Papers from the Fifth International Conference on *The Physics of Electronic and Atomic Collisions*, pp. 32 Leningrad, 1967.
b. R. B. Norton, ESSA Technical Memorandum IERTM-ITSA 60, (1967).
2. W. L. Wiese, M. W. Smith and B. M. Glennon, *Atomic Transition Probabilities*, Vol. 1, NSRDS-NBS4 (1966).
3. G. Hernandez and J. P. Turtle, *Planet. Space Sci.*, 17, 675 (1969).
4. D. M. Hunten and M. B. McElroy, *Rev. Geophys.* 4, 303 (1966).
5. L. Wallace and M. B. McElroy, *Planet Space Sci.* 14, 677 (1966).
6. J. F. Noxon, *Space Sci. Rev.* 8, 92 (1968).
7. K. A. Dick, *J. Geophys. Res.* 75, 5605 (1970).
8. W. G. Fastie, *Applied Optics*, 6, 397 (1967).
9. R. E. Miller, W. G. Fastie, and R. C. Isler, *J. Geophys. Res.* 73, 3353 (1968).
10. K. Thoebald, and H. M. Peek, Scientific Report No. LA-3929, Los Alamos Scientific Laboratory (1969).
11. S. N. Foner and R. L. Hudson, *J. Chem. Phys.* 37, 1662 (1962).
12. Y. Tanaka, A. Jursa, and F. LeBlanc, *The Threshold of Space*, M. Zelikoff Ed., Pergamon, London, (1957) p. 89.
13. J. F. Noxon, *J. Chem. Phys.*, 36, 926 (1962).
14. F. A. Morse and F. Kaufman, *J. Chem. Phys.* 42, 1785 (1965).
15. K. M. Evenson and H. E. Radford, *Phys. Rev. Lett.*, 15, 916 (1965).

16. G. Black, T. G. Slanger, G. A. St. John, and R. A. Young, J. Chem. Phys., 51, 116 (1969).
17. K. H. Welge, J. Chem. Phys., 45, 166 (1966).
18. C. L. Lin and F. Kaufman, papers presented at DASA Symposia on the Physics and Chemistry of the Upper Atmosphere, Stanford Research Institute, June 1969 and Philadelphia, June 1970.
19. R. B. Norton and C. A. Barth, J. Geophys. Res. 75, 3903 (1970).
20. D. F. Strobel, D. M. Hunten, and M. B. McElroy, J. Geophys. Res. 75, 4307 (1970).
21. a. C. A. Barth, Ann. Geophys. 22, 198 (1966); Planet. Space Sci. 14, 623 (1966).
b. L. G. Meira, J. Geophys. Res. 76, 202 (1971).
22. C. L. Lin, D. A. Parkes and F. Kaufman, J. Chem. Phys. 53, 3896 (1970).
23. A. C. G. Mitchell and M. W. Zemansky, "Resonance Radiation and Excited Atoms" Cambridge University Press, Cambridge, 1934, p. 122, 323.
24. G. M. Lawrence and B. D. Savage, Phys. Rev. 141, 67 (1966).
25. F. Labuhn, Z. Naturforschg. 20a, 998 (1965).
26. R. W. Huggins and J. H. Cahn, J. Applied Phys. 38, 180 (1967).
27. M. Cher and C. S. Hollingsworth, in *Chemical Reactions in Electrical Discharges*, pp. 118, ACS Advances in Chemical Series 80 (1969).
28. E. E. Ferguson, F. C. Fehsenfeld and A. L. Schmeltekopf, *Advances in Atomic and Molecular Physics*, Vol. 5, pp. 1, (1969).
29. R. C. Bolden, R. S. Hemsworth, M. J. Shaw and N. D. Twiddy, J. Phys. 3, 61 (1970).
30. A. L. Farragher, Trans. Faraday Soc. 66, 1411 (1970).
31. J. E. Morgan and H. I. Schiff, Can. J. Chem. 42, 2300 (1964).
32. C. B. Kretschmer and H. L. Petersen, J. Chem. Phys. 39, 1772 (1964).
33. C. H. Dugan, J. Chem. Phys. 47, 1512 (1967).
34. a. K. L. Wray, J. Chem. Phys. 44, 623 (1966).
b. R. A. Young and G. St. John, J. Chem. Phys. 48, 895 (1968).
c. J. A. Meyer, D. W. Setser, and D. H. Stedman, J. Phys. Chem. 74, 2238 (1970).

35. M. Cher and C. S. Hollingsworth, Can. J. Chem. 47, 1937 (1969).
36. W. E. Wilson, J. Chem. Phys. 46, 2017 (1967).
37. K. Schofield, Planet. Space Sci. 15, 643 (1967).
38. G. B. Kistiakowsky and G. G. Volpi, J. Chem. Phys. 27, 1141 (1957).
39. J. T. Herron and R. E. Huie, J. Phy. Chem. 72, 2235 (1968).

Table 1. First order rate constants for $N(^2D)$ decay at different pressures of Ar; $T \approx 300^\circ K$.

P (Torr)	k^I (sec^{-1})	$k^I P$ (torr sec^{-1})
15.0	215	3225
13.9	224	3105
13.0	236	3060
12.0	251	3010
10.8	275	2970
9.5	318	3015
7.9	377	2975
5.8	495	2875
4.4	665	2925
3.4	805	2725

Table 2. First-order rate constants for $N(^2D)$ decay at different pressures of He; $T \approx 300^\circ K$

P (Torr)	k^I (sec^{-1})	$k^I P$ (Torr sec^{-1})
15.8	518	8200
13.3	578	7700
11.2	700	7850
10.1	815	8200
8.8	892	7850
6.8	1160	7900
5.1	1640	8350
Average 8000		

Table 3 First order rate constants for $N(^2P)$ decay at different pressures of Ar; $T \approx 400^\circ K$.

P (Torr)	k^I (sec^{-1})	$k^I P$ (Torr sec^{-1})
15.0	408	6120
13.0	433	5620
12.0	453	5430
10.8	462	4990
9.5	475	4500
7.9	513	4050
5.9	665	3920
4.4	805	3540
3.3	1050	3460

Table 4 Rate constants (cm^3/sec) for reactions of $\text{N}(^2\text{D})$ with various gases

(Simple Planar Flow Model)				
Reactant	Diluent Gas		Corrected	Black <i>et al.</i> ¹⁶
	He	Ar		
O ₂	4.5x10 ⁻¹²	4.9x10 ⁻¹²	(6 <u>±</u> 2)x10 ⁻¹²	7x10 ⁻¹²
N ₂ O	2.2x10 ⁻¹²	3.1x10 ⁻¹²	(3.5 <u>±</u> 1.2)x10 ⁻¹²	3x10 ⁻¹²
CO ₂	2.6x10 ⁻¹³	4.6x10 ⁻¹³	(5 <u>±</u> 2)x10 ⁻¹³	6x10 ⁻¹³
NO		5.3x10 ⁻¹¹	(7 <u>±</u> 2.5)x10 ⁻¹¹	1.8x10 ⁻¹⁰
N ₂	~1x10 ⁻¹⁴	~1.5x10 ⁻¹⁴	(1.6 <u>±</u> 0.7)x10 ⁻¹⁴	≤ 6x10 ⁻¹⁵
Ar		~6x10 ⁻¹⁷	(1 <u>±</u> 0.6)x10 ⁻¹⁶	≤ 2x10 ⁻¹⁶
He	≤ 1x10 ⁻¹⁶		≤ 1.6x10 ⁻¹⁶	≤ 2x10 ⁻¹⁶

FIGURE CAPTIONS

- Figure 1. Light source and absorption cell. A-absorption cell;
W - MgF_2 windows.
- Figure 2. Decay curves for $\text{N}(^2\text{D})$ at various Ar pressures. $T = 300^\circ\text{K}$.
- Figure 3. $k^I P$ vs. P^2 for $\text{N}(^2\text{D})$ in Ar.
- Figure 4. Decay curves for $\text{N}(^2\text{D})$ at various partial pressures of N_2 ;
 $P_{\text{He}} = 14.7$ Torr; $T = 300^\circ\text{K}$.
- Figure 5. k^I vs. P_{N_2} ; $P_{\text{He}} = 14.7$ Torr; $T = 300^\circ\text{K}$.
- Figure 6. Decay of $\text{N}(^2\text{D})$ as function of added O_2 concentration;
(a) $P_{\text{He}} = 14.8$ Torr; $t = 1.85\text{msec}$;
(b) $P_{\text{Ar}} = 14.8$ Torr; $t = 1.96\text{msec}$.
- Figure 7. Decay of $\text{N}(^2\text{D})$ as function of added N_2O concentration;
(a) $P_{\text{He}} = 14.6$ Torr; $t = 1.80\text{msec}$;
(b) $P_{\text{Ar}} = 6.8$ Torr; $t = 2.25\text{msec}$.
- Figure 8. Decay of $\text{N}(^2\text{D})$ as function of added CO_2 concentration;
(a) $P_{\text{He}} = 14.5$ Torr; $t = 1.80\text{msec}$;
(b) $P_{\text{Ar}} = 12.8$ Torr; $t = 1.98\text{msec}$.
- Figure 9. Decay of $\text{N}(^2\text{D})$ as function of added NO concentration integrated over reaction time of 2.0msec ; $P_{\text{Ar}} = 12.8$ Torr;
 $[\text{N}] = 1.27 \times 10^{14} \text{cm}^{-3}$.
- Figure 10. O-atom production in $\text{N}(^2\text{D}) + \text{O}_2$ as function of added O_2 concentration; $P_{\text{Ar}} = 13$ Torr; $t = 2.02\text{msec}$.
- Figure 11. Corrected O-atom production and initial $\text{N}(^2\text{D})$ concentration.

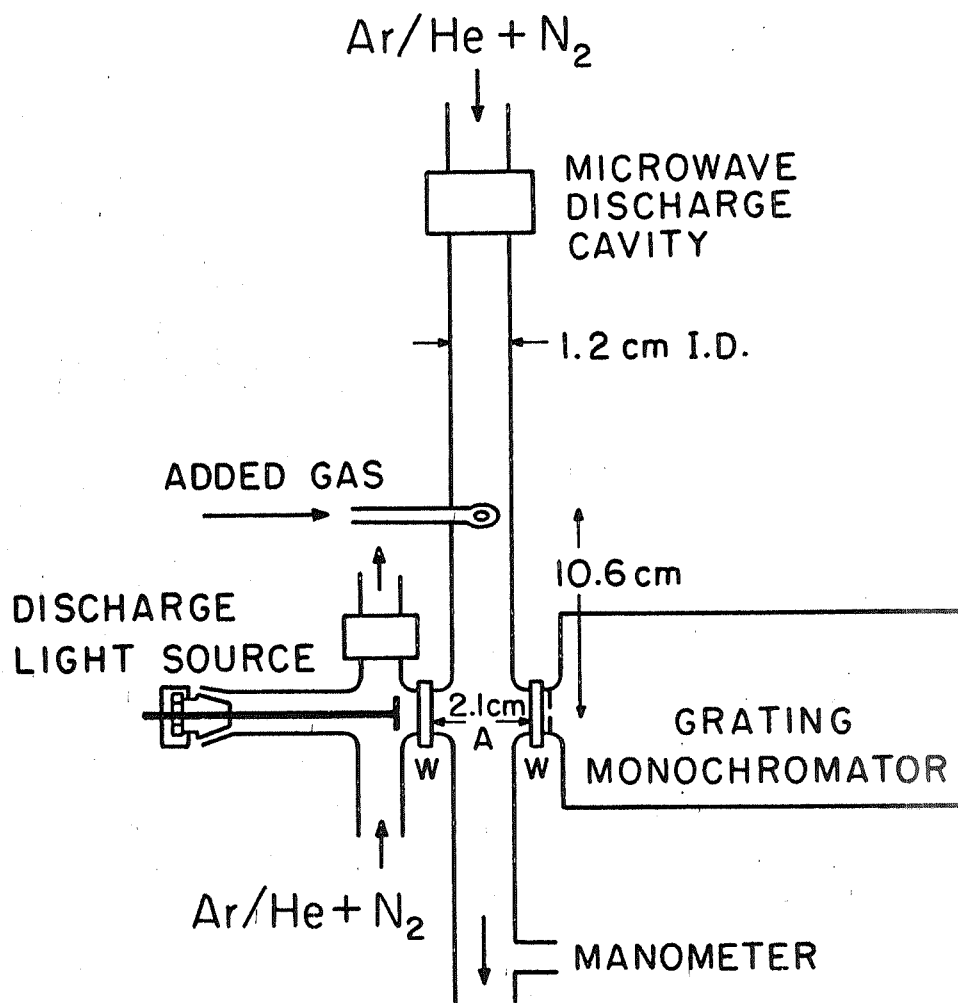


Figure 1

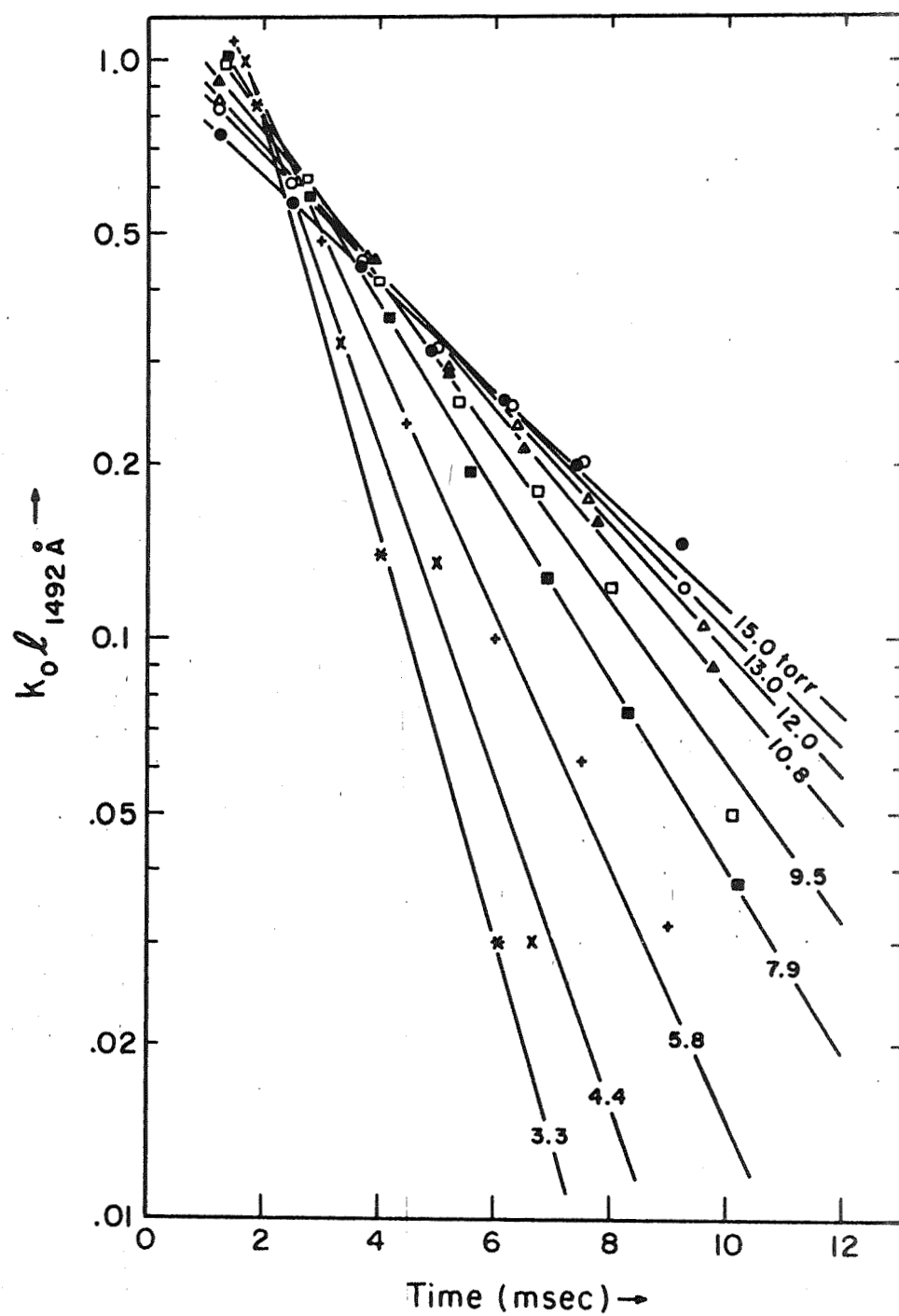


Figure 2

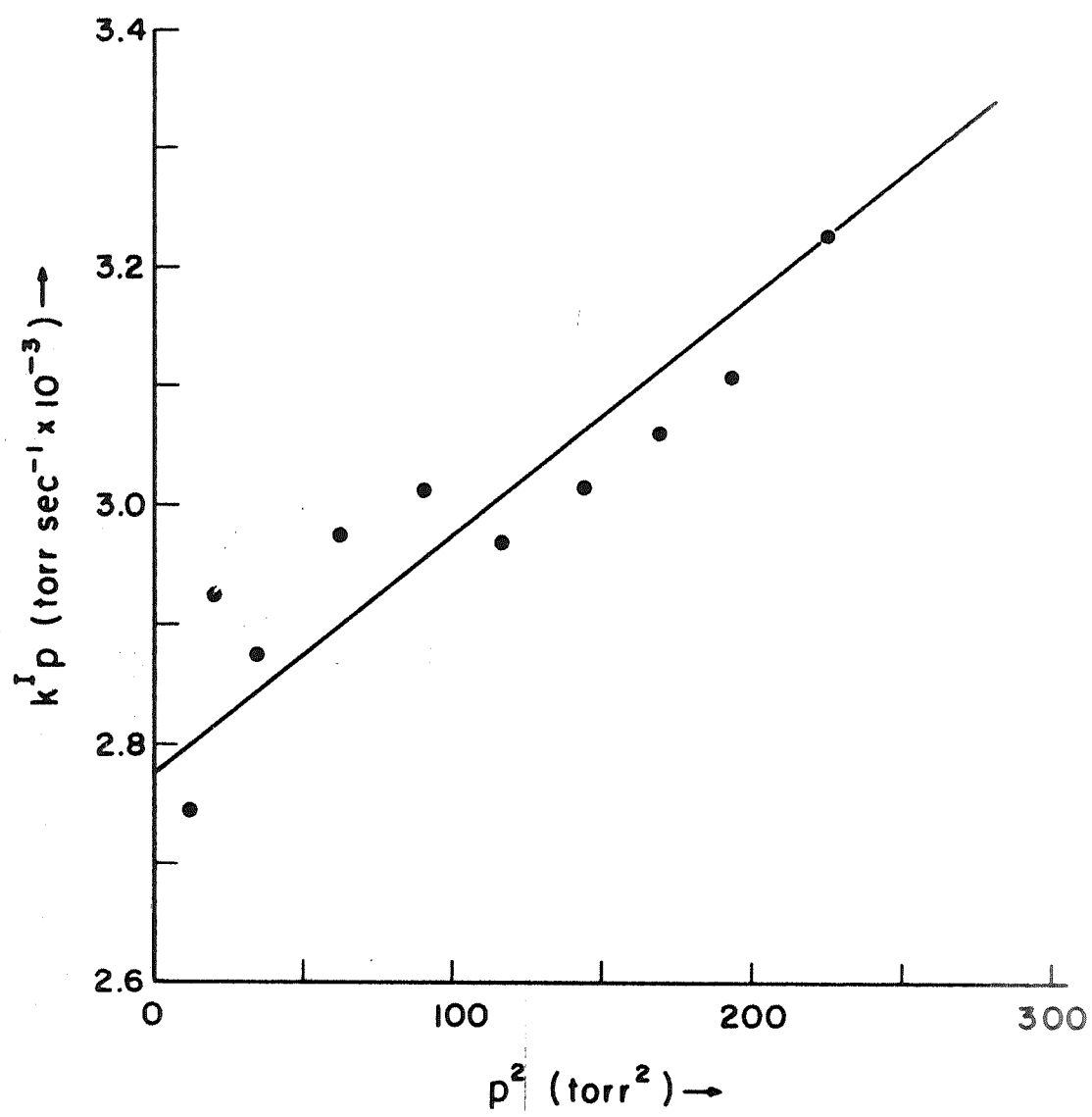


Figure 3

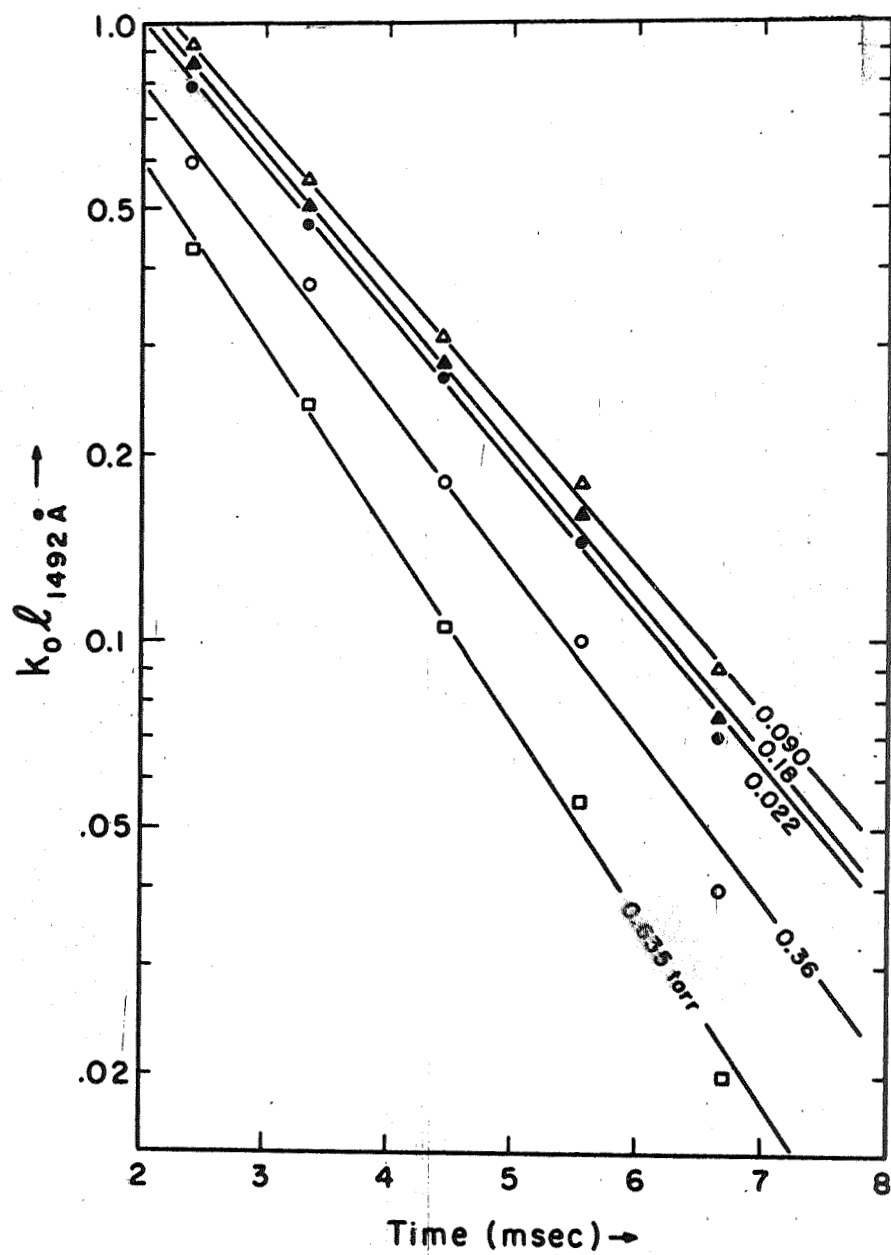


Figure 4

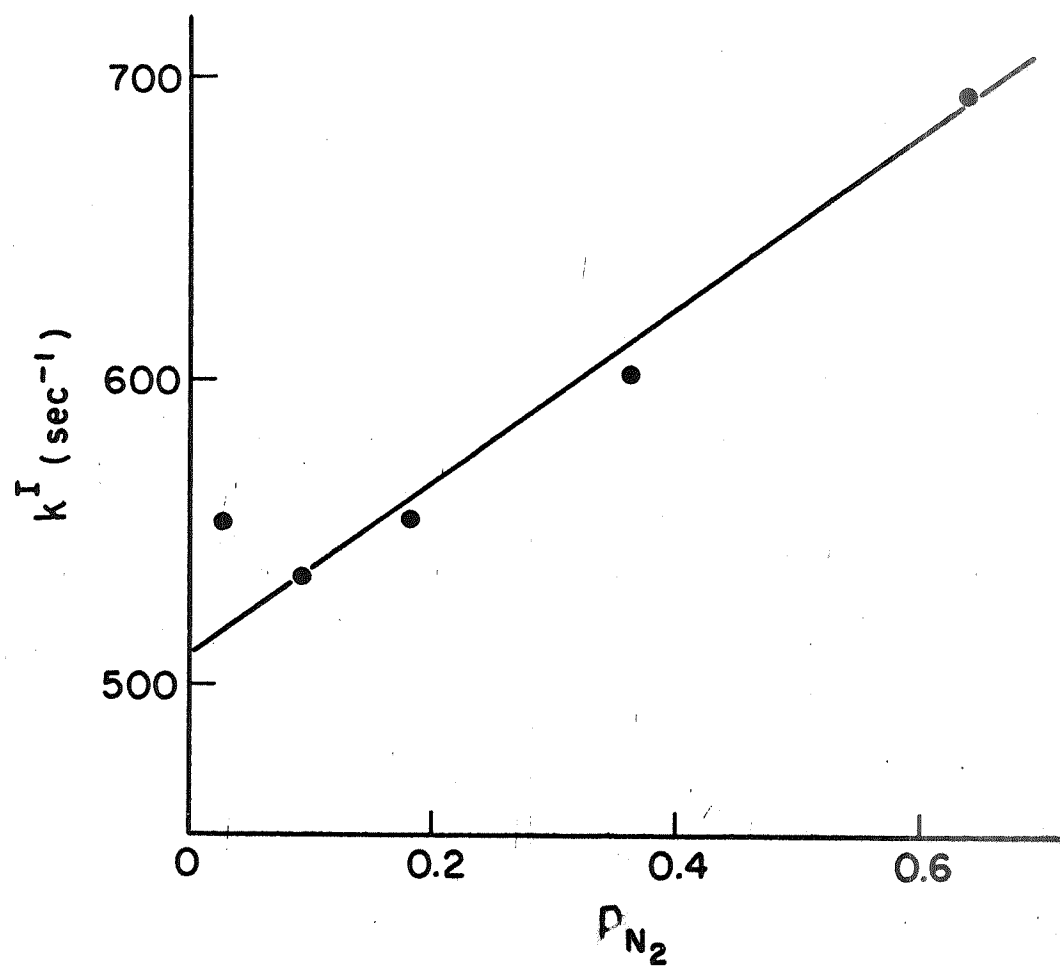


Figure 5

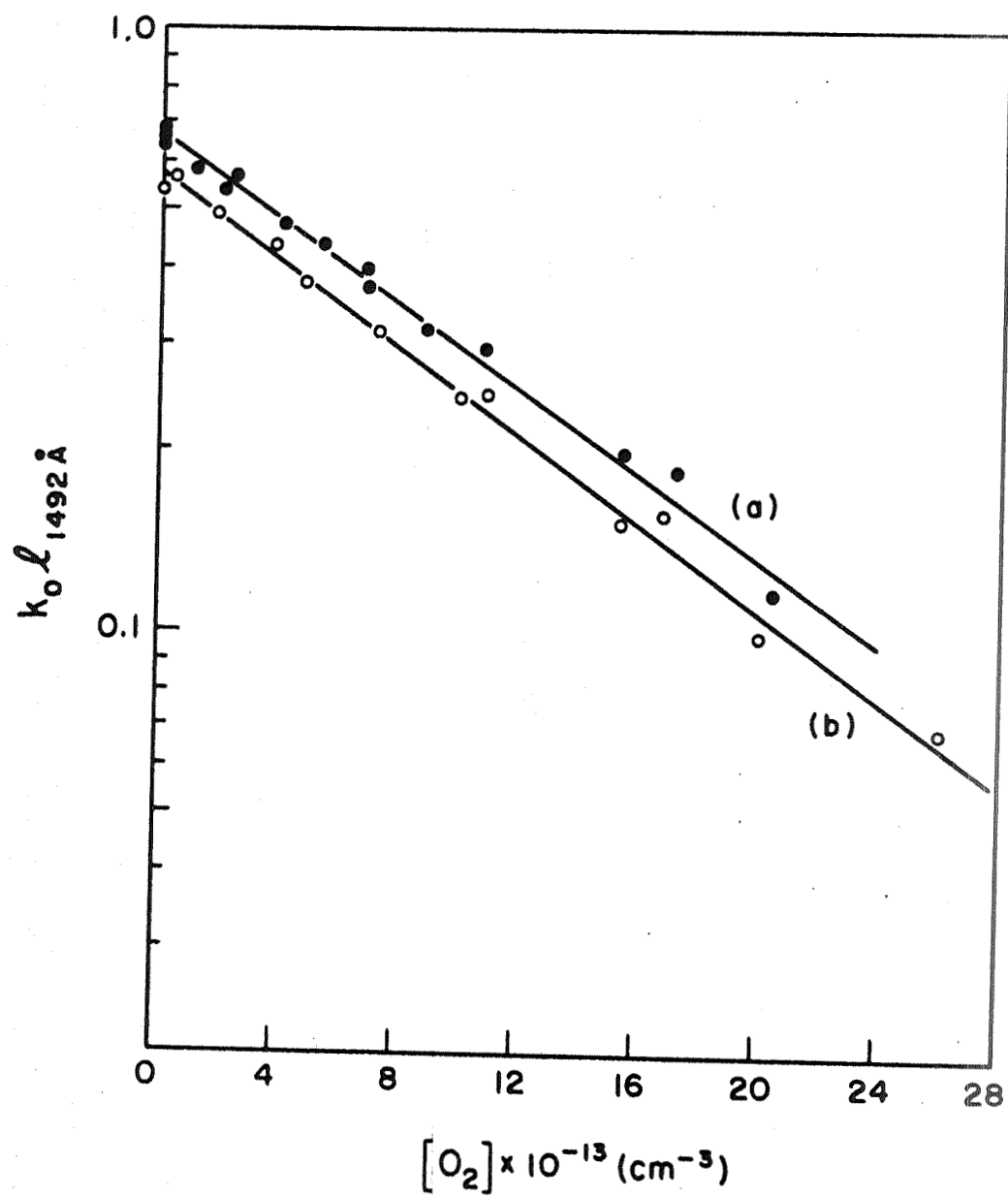


Figure 6

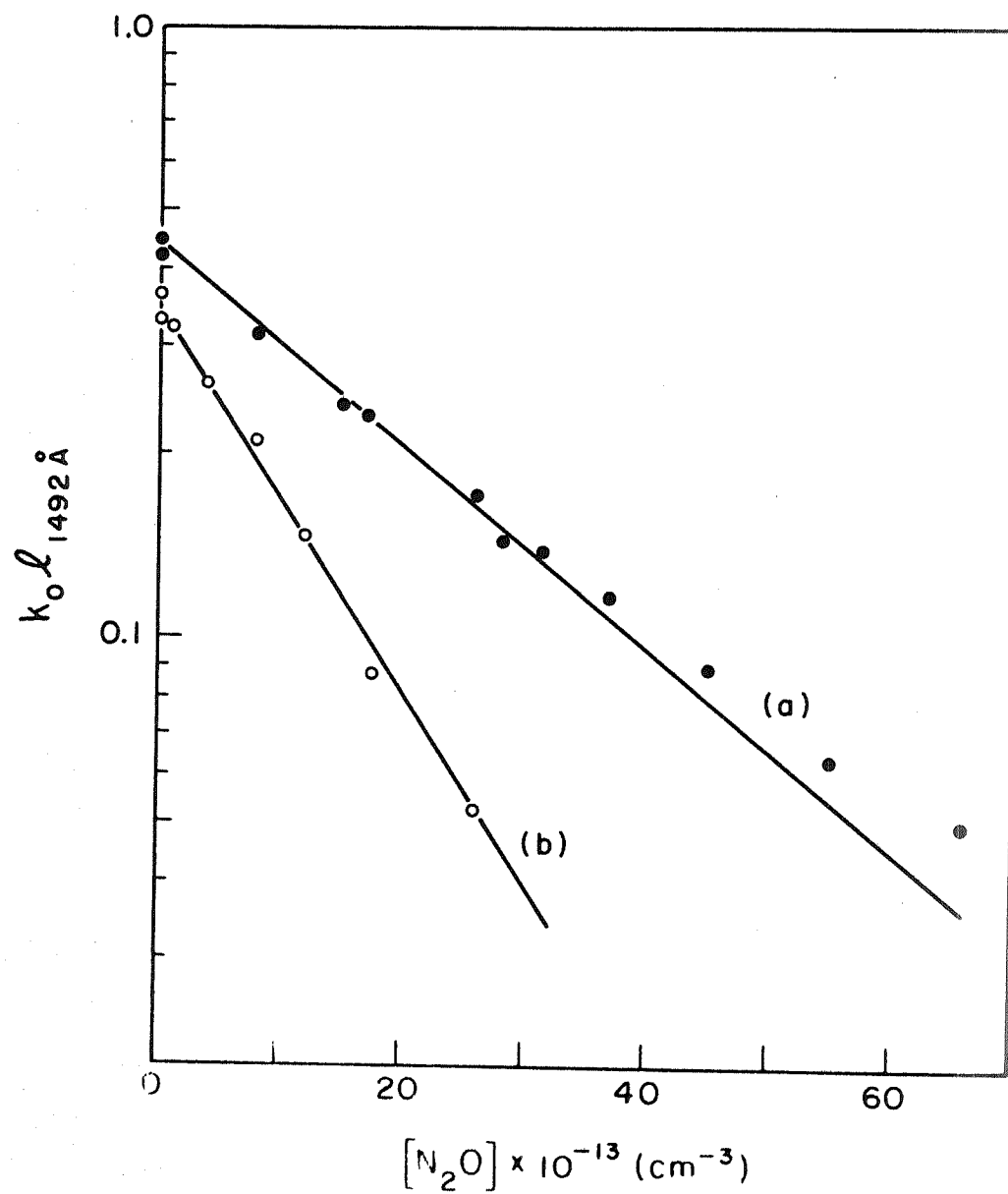


Figure 7

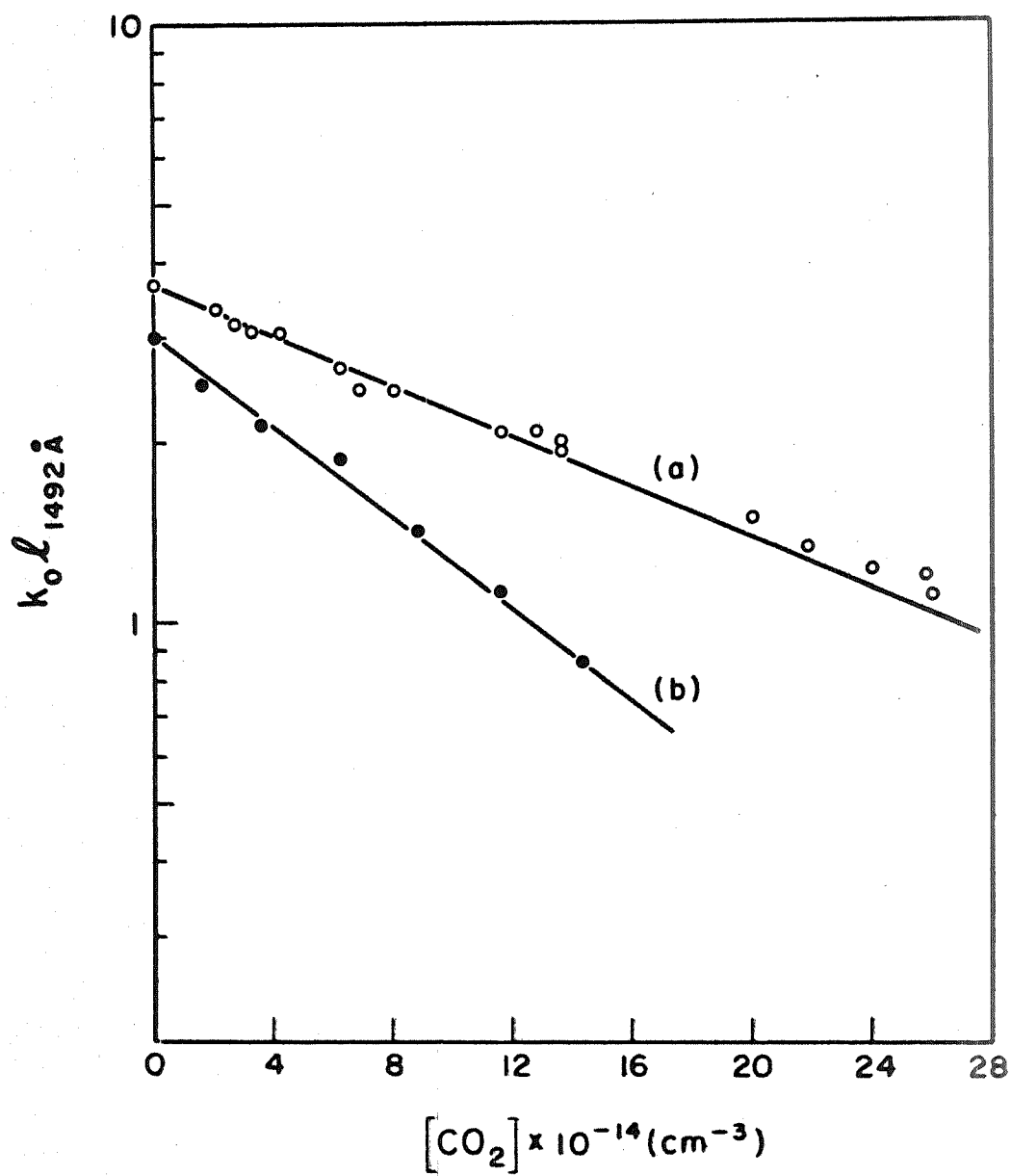


Figure 8

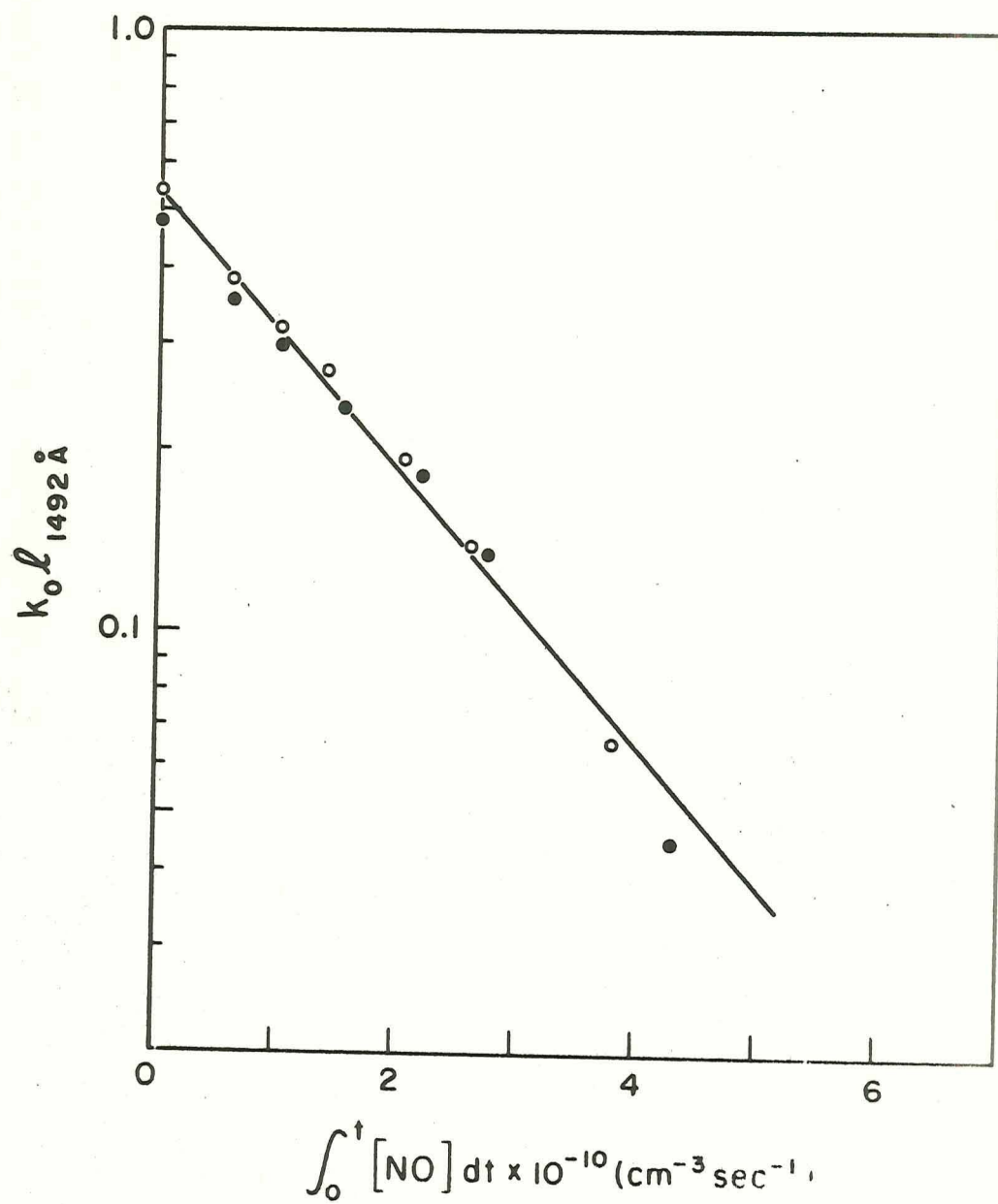


Figure 9

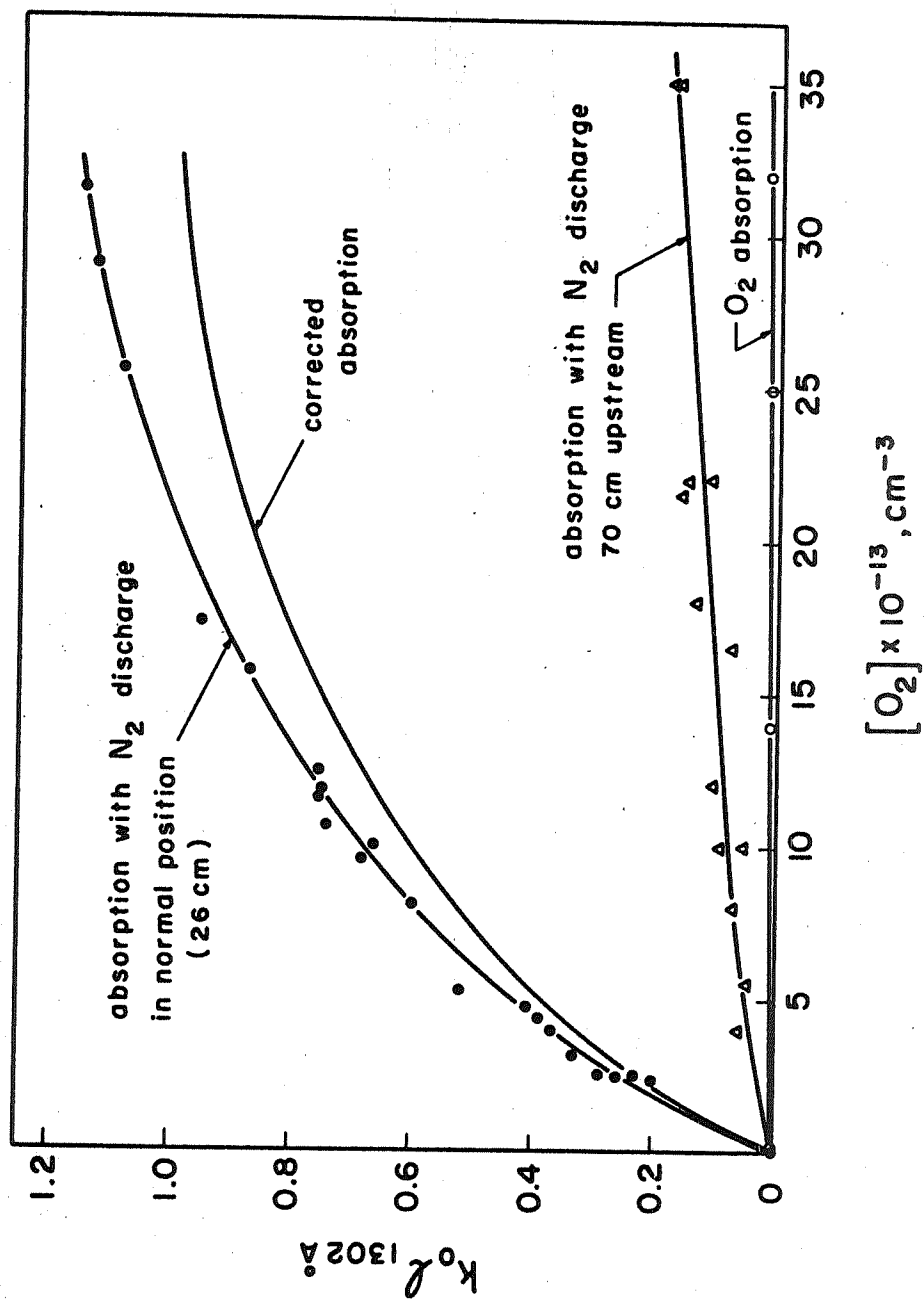


Figure 10

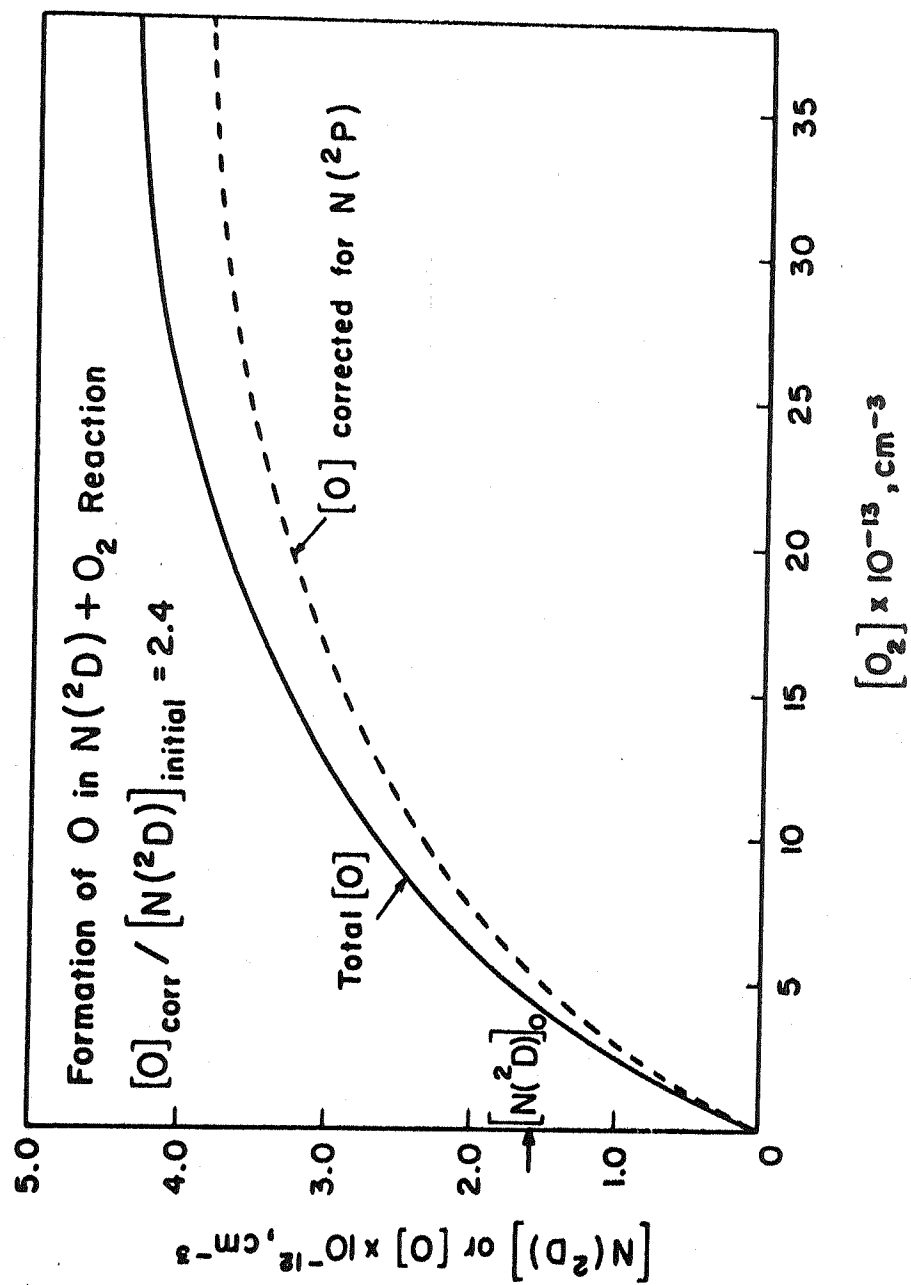


Figure 11